
CONTENTS

	<i>2N bound state</i>
1	Introduction
	<i>and</i>
2	Formalism & numerical methods
2.1	Deuteron bound state
2.2	2N scattering state
2.3	3N bound state
2.4	3N scattering state
2.5	Nd scattering state
2.6	Nuclear electromagnetic current
2.7	Pion absorption
2.8	Theoretical uncertainties
3	Results
3.1	Deuteron photodisintegration
3.1.1	Cross section
3.1.2	Polarization observables
3.2	Helium photodisintegration
3.2.1	3N photodisintegration
3.2.2	D-p photodisintegration
3.3	Triton photodisintegration
3.4	Pion absorption from the lowest atomic orbital
3.4.1	Pion absorption in ^2H
3.4.2	Pion absorption in ^3He
3.4.3	Pion absorption in ^3H
4	Summary
	Bibliography

Abstract



Lorem ipsum dolor sit amet, consectetur adipiscing elit, sed do eiusmod tempor incididunt ut labore et dolore magna aliqua. Ut enim ad minim veniam, quis nostrud exercitation ullamco laboris nisi ut aliquip ex ea commodo consequat. Duis aute irure dolor in reprehenderit in voluptate velit esse cillum dolore eu fugiat nulla pariatur. Excepteur sint occaecat cupidatat non proident, sunt in culpa qui officia deserunt mollit anim id est laborum.

CHAPTER 1

INTRODUCTION

Why we study few nucleon systems

The study of light nuclei and their reactions has been serving as an easy way to investigate particles in nuclei and the forces between them for decades. A convenient way to proceed may be to study the interaction of a nucleus with other nuclei, particles, or electroweak probes such as electrons, photons, muons, pions, neutrinos, and hyperons. In most cases, study of elastic or inelastic scattering is possible. This can be done either theoretically or by performing relevant experiments to test if the theory works. It should be taken into account that nuclear interactions may be caused by different fundamental forces, including strong, weak, or electromagnetic interactions. This depends on the type of particle being scattered and the target of the reaction and requires different theoretical approaches. Of course gravitational force is also in the game but due to its weakness it is usually omitted in the nuclear physics.

In the past many experimental efforts have been undertaken and experimentalists have been interested in electromagnetic reactions involving light nuclei for decades. There are experimental data from the second half of 20th century (e.g. [1–4]) which are still useful for comparing theoretical predictions with experimental measurements. There are several facilities providing sources of gamma rays (both low- and high-energy) and other particles that have been operating for decades and still enable experiments to be conducted. Let us mention here such facilities as TUNL with HI γ S [5, 6], MAMI [7].

To accurately describe nuclear reactions, two important components of the Hamiltonian must be considered. They are nuclear interactions and nuclear currents. First of all, various nuclear forces may act on the particles.

The strong nuclear force acts inside the nuclei and, among others, bound neutrons and protons together. The description of strong interactions is extremely difficult as it deals not only with the nucleons themselves, but also with their constituents: quarks and gluons. Quantum chromodynamics (QCD) is a modern theory describing strong interactions, but, at the moment, it is not applicable at low energies (e.a. at $Q^2 \lesssim 1\text{GeV}^2$). In such situation various approaches are emerging. The most advanced are the chiral effective theory and lattice calculation [8–10]. In this work we will use results of the first approach and corresponding model is described in Sec. 2.

Study of three- (and more) nucleon systems showed that the strong two-nucleon (2N) force is not efficient in describing $N > 2$ systems, thus a 3N force was introduced. The

first applications of such a force showed that it brings a sizable contribution to observables and cannot be ignored [11]. The contribution of the 3NF can be examined by comparing binding energies of light nuclei calculated with and without this part of Hamiltonian with respect to experimental values.

For example, the binding energy for ${}^3\text{H}$ calculated with the Argonne V18 (AV18) 2N potential without 3NF amounts to $E_b({}^3\text{H}) = -7.628 \text{ MeV}$ [12]. There are different models that might add a 3NF contribution to AV18 (or other potentials). Using the Tucson-Melbourne (TM) model [13] results in $E_b({}^3\text{H}) = -8.478 \text{ MeV}$, and Urbana IX [11] 3NF provides us with $E_b({}^3\text{H}) = -8.484 \text{ MeV}$. Looking at the experimental value $E_b({}^3\text{H}) = -8.482 \text{ MeV}$, it is clear that the 3NF contribution makes the prediction much closer to the measurement. Nevertheless, the parameters of the UrbanaIX 3NF were fitted to the experimental value for ${}^3\text{H}$, so there is no surprise in good agreement.

However one can also check the binding energy for other nuclei, which were not used for the fitting. The ~~2NF~~ binding energy for ${}^3\text{He}$ (calculated with ~~the~~ AV18) is $E_b({}^3\text{He}) = -6.917 \text{ MeV}$. ~~The~~ TM contribution makes it $E_b({}^3\text{He}) = -7.706 \text{ MeV}$, ~~Urbana IX gives~~ $E_b({}^3\text{He}) = -7.739 \text{ MeV}$, while the experimental value is $E_b({}^3\text{He}) = -7.718 \text{ MeV}$. One can see the importance of 3NF contribution also for the α -particle's (${}^4\text{He}$) binding energy: AV18 alone gives $E_b({}^4\text{He}) = -24.25 \text{ MeV}$, while AV18 – TM leads to -28.84 MeV , AV18 – Urbana IX delivers $E_b({}^4\text{He}) = -28.50 \text{ MeV}$, and the experimental value is -28.30 MeV [12].

Whereas the first applications included only early simplified "realistic" 3N potential, the latter investigations, based on more advanced models, fully confirmed this statements [15, 16]. Within new models the four-nucleon (4N) interaction was constructed to improve description of ${}^4\text{He}$ [17]. Broader discussion of nuclear forces used in this thesis is given below.

partons Electromagnetic force appears between charged particles like protons, electrons or pions. That force acts also between charged particles and photons, so in photon- and electron- scatterings on the nuclei it is a necessary component of a description. However, electromagnetic interaction between ~~nucleons~~ particles manifests only at very low energies or for specific kinematic configurations with two ~~photons~~ having approximately equal momenta. Thus it rather is being skipped in lowest order analysis.

The main contribution of electromagnetic interaction to disintegration processes in hand is due to the current ~~operator~~ operator describing photon-nucleon vertex. The structure of the electromagnetic current have been investigated in many works by numerous groups [18] but it was H. Arenhövel who performed study of nuclear electromagnetic current in few-nucleon sector. His long-term research, reviewed in [19] demonstrated various theoretical models applied to the deuteron photodisintegration. He analyzed among others a nonrelativistic potential model, a relativistic impulse approximation, and a relativistic meson-exchange model. These models were used to calculate the differential cross section and various polarization observables, which describe the probability of the process occurring at different scattering angles, photon energies, spin directions etc.

observed The calculated cross sections were then compared to experimental data, and it was found that the relativistic meson-exchange model provided the best agreement with the data at photon's energies up to $E_\gamma = \sim 100 \text{ MeV}$. At higher energies agreement is presented but is getting worse. This model includes the exchange of virtual mesons between the interacting particles, which accounts for the strong and electromagnetic forces between them.

Overall, Arenhövel demonstrated the importance of including both strong interaction

*footnote { more precisely it is a 2 ground state energy, but I follow commonly used mental shortcut. }

because you are writing
about $n \rightarrow p + e^- + \bar{\nu}_e$

and electromagnetic current operator in a description of the deuteron photodisintegration process, and highlighted the need for accurate theoretical models to interpret experimental data.

The weak force is of great importance in the study of nuclear processes. One of the main roles of the weak force is to mediate ~~check correction~~ beta decay, which is a process in which a neutron in a nucleus is converted into a proton, emitting an electron and an antineutrino. This process plays a crucial role in the formation of elements in the universe, as it allows for the conversion of neutron-rich isotopes into more stable, proton-rich isotopes. Additionally, the weak force plays a role in neutrino interactions with matter, which are of great interest in both astrophysics and particle physics. In nuclear physics, weak interactions can also play a role in the decay of unstable nuclei, the production of neutrinos in nuclear reactions, and the scattering of neutrinos off nuclei. The study of weak interactions is therefore an essential component of the overall understanding of nuclear physics and the behavior of matter on the subatomic scale. However, in the thesis we stick up with electromagnetic processes.

Models of strong interaction used in the thesis

In order to model the nuclear potential, physicists often use phenomenological or semi-phenomenological approaches. It allows them to combine theoretical knowledge about the studied processes and experimental findings.

Among many of such models, the AV18 [10] force is one of most advanced and therefore is used in current thesis. In order to construct the nucleon-nucleon (NN) force, authors combine one-pion-exchange part with phenomenological one and supplement them by electromagnetic corrections. Free parameters were fitted to the Nijmegen partial-wave analysis of pp and np data [20]. Authors showed, that the AV18 potential delivers good description of nucleon scattering data ($\chi^2/\text{data} = 1.08$ for around 4000 pp and np scattering datasets) as well as deuteron properties (estimated binding energy is 2.2247(35) MeV vs experimental 2.224 575(9) MeV). [] do we have a reference?

Weinberg's idea of using chiral symmetry to describe nuclear interactions at low energies was first introduced in his papers published in 1990 and 1991 [21, 22]. In these papers, Weinberg argued that the low-energy dynamics of nucleons could be described using a chiral Lagrangian, which is the most general Lagrangian consistent with chiral symmetry and its spontaneous breaking. This Lagrangian is expressed in terms of nucleon and pion fields, which are the degrees of freedom that become relevant at low energies.

The chiral Lagrangian is the starting point for the development of the Chiral Effective Field Theory (χ EFT), which has become one of the most advanced approaches to low-energy nuclear physics [23]. The use of the χ EFT allows (at least in theory) for the calculation of nuclear properties and reactions in a model-independent way. It is also possible to quantify the uncertainties associated with the calculation. One of the key features of the χ EFT is that it allows for the construction of a nuclear potential, which can then be used in relevant formalisms, e.g. to solve the Schrödinger equation and to obtain bound and scattering states properties. The accuracy of the potential can be systematically improved by including higher-order terms in the chiral expansion, which leads to a better description of experimental data.

In the χ EFT there are two natural scales: so-called soft scale $Q \sim M_\pi$ - the mass of pion and the hard scale - $\Lambda_\chi \sim 0.7 \text{ GeV}$ - the chiral symmetry breaking scale. The ratio between these two scales Q/Λ_χ is being used as an expansion parameter in χ EFT with

power ν : $(Q/\Lambda_\chi)^\nu$.¹

Possibility of deriving nuclear potential is an important feature of χ EFT. The potential, as occurs in Lagrangian, is a perturbation expression of the same parameter Q/Λ_χ . Considering so-called irreducible diagrams (which cannot be split by cutting nucleon lines), Weinberg [21, 22] came to the expression for the powers ν_W of such diagrams

$$\nu_W = 4 - A - 2C + 2L + \sum_i \Delta_i, \quad (1.1)$$

where i specifies a vertex number and

$$\Delta_i \equiv d_i + \frac{n_i}{2} - 2. \quad (1.2)$$

In Eq. (1.1) C is a number of pieces which are connected, L - the number of loops in the graph and A is a number of nucleons in the diagram. In Eq. (1.2) n_i is a number of nucleon field operators and d_i - the number of insertions (or derivatives) of M_π .

The further analysis of Eq. (1.1) revealed some problems which occur for particular values of parameters in the equation, namely negative values of ν_W are possible while the order has to take integer values from 0 to infinity. In order to deal with that, Eq. (1.1) was slightly modified by adding $3A - 6$ to it [10, 26]:

$$\nu = \nu_W + 3A - 6 = -2 + 2A - 2C + 2L + \sum_i \Delta_i. \quad (1.3)$$

That convention above is widely used and we will also stick to it as well.

*2NF fine
(if you have
removed
interaction in
fig 2)*

In χ EFT the first order, "leading order" ($\nu = 0$) is followed by the next-to-leading order ($\nu = 2$)², the next-to-next-to-leading order ($\nu = 3$) and so on. At each chiral order, new interaction diagrams complete the potential. There are only two diagrams at leading order (LO): one is a contact term and the other one is a one-pion exchange, see Fig. 1.1. Both diagrams reflect only 2NF. The same is for diagrams at next-to-leading order (NLO), where more contact terms occur together with two-pion exchange topologies. Each subsequent order includes more and more sophisticated diagrams describing nucleons interaction via multiple pion exchanges and various contact vertices. 3NF appears for the first time at next-to-next-to-leading order (N^2LO) while 4NF contributions start from next-to-next-to-next-to-leading order (N^3LO). This scheme establishes for the first time a systematic way to include all the contributions to a strong nuclear force starting from the simplest diagrams at LO and gradually adding more and more terms. It is also beneficial in the way that one can obtain results using chiral potential at different orders and track which one gives large or small contribution to the final prediction. At the moment, next-to-next-to-next-to-next-to-leading order (N^4LO) is the highest order at which 2N interaction has been completely derived. Nevertheless leading F-wave contact interactions from N^5LO have been combined with N^4LO force leading to the N^4LO^+ potential, which is currently regarded as a best available potential on the market. The progression of the chiral orders is reflected in a $\chi^2/data$. Leading order results in $\chi^2/data = 73$ (with neutron-proton data with $E_{lab} = 0 - 100\text{MeV}$). Each subsequent order has better and better results: NLO gives $\chi^2/data = 2.2$, N^2LO - $\chi^2/data = 2.2$ and the highest, N^4LO^+ ,

¹Note that exact values of some parameters are still under discussion [24]. We follow here approach proposed by E.Epelbaum and collaborators, see e.g. [25]

²The contributions to the potential at order $\nu = 1$ completely vanish due to parity and time-reversal invariance, so the next-to-leading order stands for the second order ($\nu = 0$) of expansion.

leads to $\chi^2/\text{data} = 1.08$ [25]. Similar progress is observed for wider energy range, e.g. for $E_{\text{lab}} = 0 - 300 \text{ MeV}$ χ^2/data is 75, 14, 4.2, 2.01, 1.16 and 1.06 at LO, NLO, N²LO, N³LO, N⁴LO and N⁴LO⁺, respectively. The proton-proton data description has similar trend, so χ^2/data is 1380, 91, 41, 3.43, 1.67, 1.00 for the same energy bin and chiral orders. At N⁴LO⁺ χ^2/data for proton-proton data stands similar value (close to 1) as for neutron-proton, but the convergence comes a bit later and leading order has way worse description. In my work I will use chiral potentials from LO up to N⁴LO⁺.

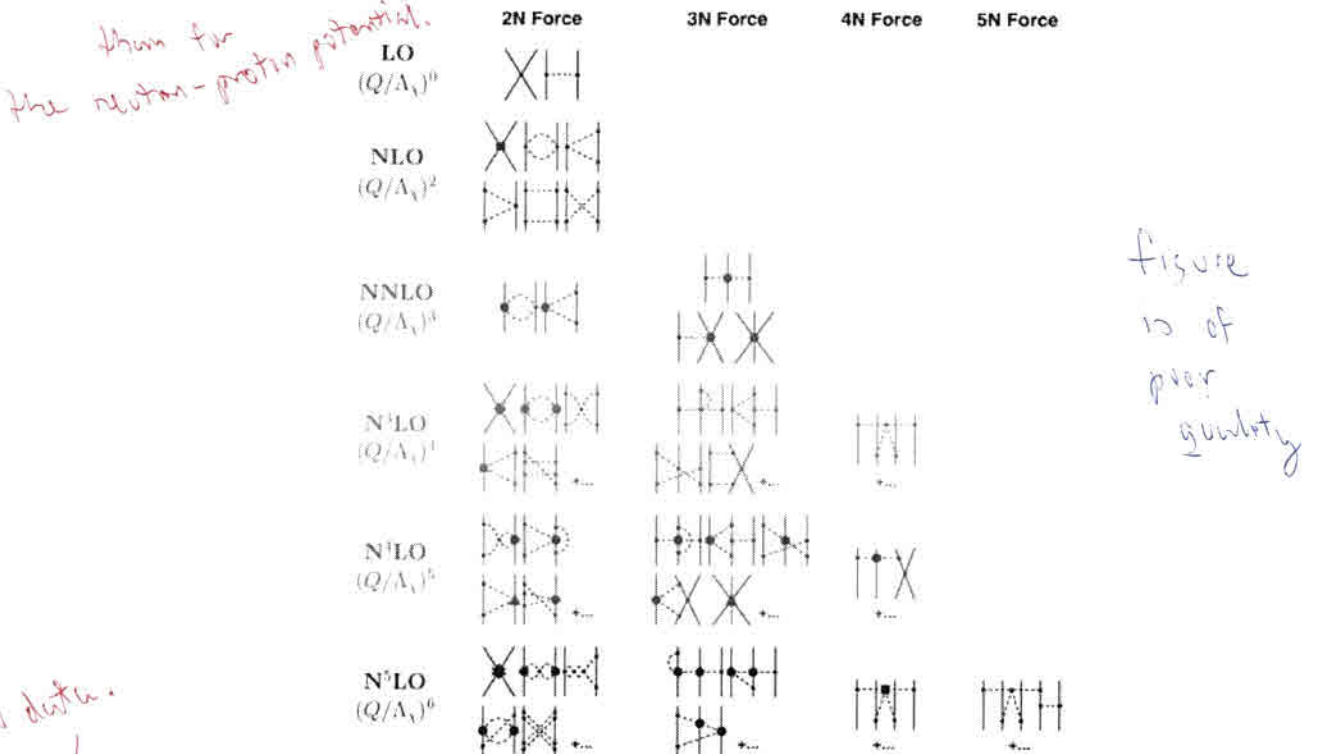


Figure 1.1: Make own diagrams, e.g. with JaxoDraw or PyFeyn [17]

The Argonne V18 potential [16], mentioned earlier, has 40 adjustable parameters, while χ EFT NN potential at N⁴LO [10] has only three ~~parameters~~ low-energy constants (LECs) fitted to deuteron properties. The reduction of the number of free parameters of the χ EFT-based potentials has not only a theoretical but also a practical advantage in the studies of nuclear systems.

The general scheme outlined above was developed mainly by the Bochum-Bonn and Moscow-Idaho groups. Both groups have similar approaches and were independently and almost simultaneously developing their models. In 1998 Epelbaum and collaborators from the Bochum-Bonn group presented a first version of their NN chiral potential [28, 29]. Developing a more and more sophisticated versions with higher chiral orders, authors presented N³LO^{NN} potential in 2005 [30] which included a 3NF contributions. They were further developing their chiral model, taking into account more Feynmann diagrams coming to a higher chiral orders. At some moment Bochum-Bonn group faced with a problem of potential regularisation [31, 32]. Solving it was an important step and authors where struggling with finding an appropriate regularization method to handle the divergences that arise in the χ EFT calculations. Different techniques were applied such as the cutoff regularization and the regulator function methods. An important point was when authors

CHAPTER 1. INTRODUCTION

started using a semi-local regularisation in the coordinate space. The ~~correspondent~~ potential is called the SCS potential (semi-local regularisation in the coordinate space) [33]. Later similar regularisation, but done in momentum space was introduced, resulting in the most advanced chiral potential at the moment up to N^4LO^+ chiral order [25]: the semilocal momentum-space regularized potential (SMS). It is developed up to N^4LO^+ at the moment.

On the other side of the planet, in Idaho, Machleidt and his group from Moscow (Idaho) were also developing a chiral interaction. Their results from 2003 [31], following with later investigations [27, 35, 36] introduced very similar model to the one from the Bochum-Bonn group with minor technical differences.

There are a number of another attempts to construct the nuclear potential from the χ EFT. M.Piarulli et al [37, 38] contributed to quite similar approach, based on the same chiral potentials but including explicitly Δ -isobar intermediate states up to the third chiral order and taking into account sophisticated electromagnetic corrections. *advanced*

Other groups try to improve already derived forces. Let us mention here works by A. Ekström and collaborators [39, 40] who, by using ~~sophisticated~~ fitting methods combined with statistical analysis, proposed so-called optimised interaction V_{opt} which was proved to provide a good description of ~~atom~~ properties for ~~radii and calcium without~~ *and nuclear matter*

Another approach is the pionless effective field theory, which integrates out pions and focuses on the various types of contact interactions between nucleons [41]. Obtained potential has a very simple form, but cannot be applied to higher energies since pions start playing an important role there. *V-G.*

Yet another promising approach is the Lattice Effective Field Theory (LEFT), which is based on the Lattice QCD simulations of the strong interaction. Meißner and collaborators have developed a chiral effective theory for nuclear forces based on the ~~results~~ of lattice QCD calculations [42]. This approach has the advantage of being able to predict the nuclear force directly from the first principles, without the need for phenomenological input. However, currently it is limited to small systems and low energies due to the computational resources required for calculations. Up to now, the relatively simple two-nucleon scattering problem and few-nucleon bound state have been solved within the LEFT and more complex systems are still under attack. For more details please refer to [42].

Technically, the chiral potential may be derived both in coordinate and momentum spaces. Nevertheless in both cases it requires regularisation which improves potential behavior at small distances or at high momenta, which allows to avoid infinities. The SMS potential is being regularized semilocally. It means that local or nonlocal regularisations are being applied for different parts of the potential. In [30, 34] the non-local regulation scheme was applied to both short- and long-range parts of the potential while in the next model [27, 33] it affected only a short range part. This regularisation is applied directly to the potential matrix elements in the coordinate space:

$$V_\pi(\vec{r}) \rightarrow V_{\pi,R}(\vec{r}) = V_\pi(\vec{r}) (1 - \exp(-r^2/R^2)), \quad (1.4)$$

or in the momentum space

$$V_\pi(\vec{p}', \vec{p}) \rightarrow V_\Lambda(\vec{p}', \vec{p}) = V_\pi(\vec{p}', \vec{p}) \exp[-(p'/\Lambda)^{2n} - (p/\Lambda)^{2n}], \quad (1.5)$$

where the cutoff R was chosen in the range of $R = 0.8, \dots, 1.2$ fm, $\Lambda = \frac{2}{R}$ and n being

CHAPTER 1. INTRODUCTION

adjusted with respect to the considered chiral order. For specific case of the SMS force $\Lambda = 400 - 550 \text{ MeV}$ and $n = 3$.

The other way of regularisation, the local one, is applied to the propagator operator, already during the derivation of potential. Namely, the Gaussian form factor $F(\vec{l}^2)$ is being used to reduce pions with higher momenta:

$$\int_{-\infty}^{\infty} \frac{\rho(\mu^2)}{\vec{l}^2 + \mu^2} d\mu^2 \rightarrow \frac{F(\vec{l}^2)}{\vec{l}^2 + \mu^2} \quad (1.6)$$

with

$$F(\vec{l}^2) = e^{-\frac{\vec{l}^2 + M_\pi^2}{\Lambda^2}}, \quad (1.7)$$

M_π is an effective pion mass, Λ - a cutoff parameter and \vec{l} is a four-momentum of the exchanged pion. Further μ is a ... The form factor (1.7), being used together with Feynman propagator, ensures that long-range part of the forces has no singularities.

The cut-off parameter Λ is not fixed and usually calculations are being performed for its different values. The comparison of such results may reveal stronger or weaker dependence and in a perfect case, which is expected at $\nu \gg 1$, one will come up with such a potential, were the cut will not affect results at all. One of aims of my thesis is to test how big cut-off dependency of predictions is observed for the best currently available forces (SCS and SMS). To illustrate a cutoff dependency of the potential, in Fig. 1.2 I show values of the matrix elements for $2N \langle \vec{p}|V|\vec{p}' \rangle$ potential ${}^3S_1 - {}^3D_1$ as a function of the momentum $|\vec{p}|$ with fixed value $|\vec{p}'| = 0.054 \text{ fm}^{-1}$. Please note, that relatively strong dependency of specific matrix element of the potential is not always leading to a strong dependency of observables, as observables comprise contributions from many matrix elements.

Yet another regularisation function is used by R. Machleidt, D.R. Entem and A. Nogga, when regulating matrix elements of the potential in momentum space with non-local regulator only. That is a main reason of the observed differences between predictions based on Epelbaum's and Machleidt's models.

Currents

The electromagnetic current operator for a few-nucleon system has both one- and many-body contributions, which can be denoted as $j_\mu^1, j_\mu^2, j_\mu^3$, etc, respectively (where $\mu = 0..3$ denotes a four-vector components). The leading one-body contribution, j_μ^1 , represents the photon's interaction with a single nucleon. The many-body contributions are known as meson exchange currents (MEC), and arise from the meson-exchange picture of the nucleon-nucleon (NN) interaction. In that picture the photon can couple to mesons exchanged between two nucleons, leading to two-body contributions to the nuclear current. The necessity of introducing the MEC arises from the continuity equation, which requires the inclusion of two-body interactions in the Hamiltonian. The momentum and isospin-dependent terms in the potential require, in turn, the introduction of two-body MEC. Similarly, the inclusion of the three-body force into the Hamiltonian requires the existence of three-body contributions to the nuclear current. However, the effects of the three-body MEC are likely negligible in the low-energy region. Therefore, in the thesis I will consider one- and two-body currents, only. The continuity equation, connecting the interaction and the current clearly shows that those two quantities should be derived

+ two

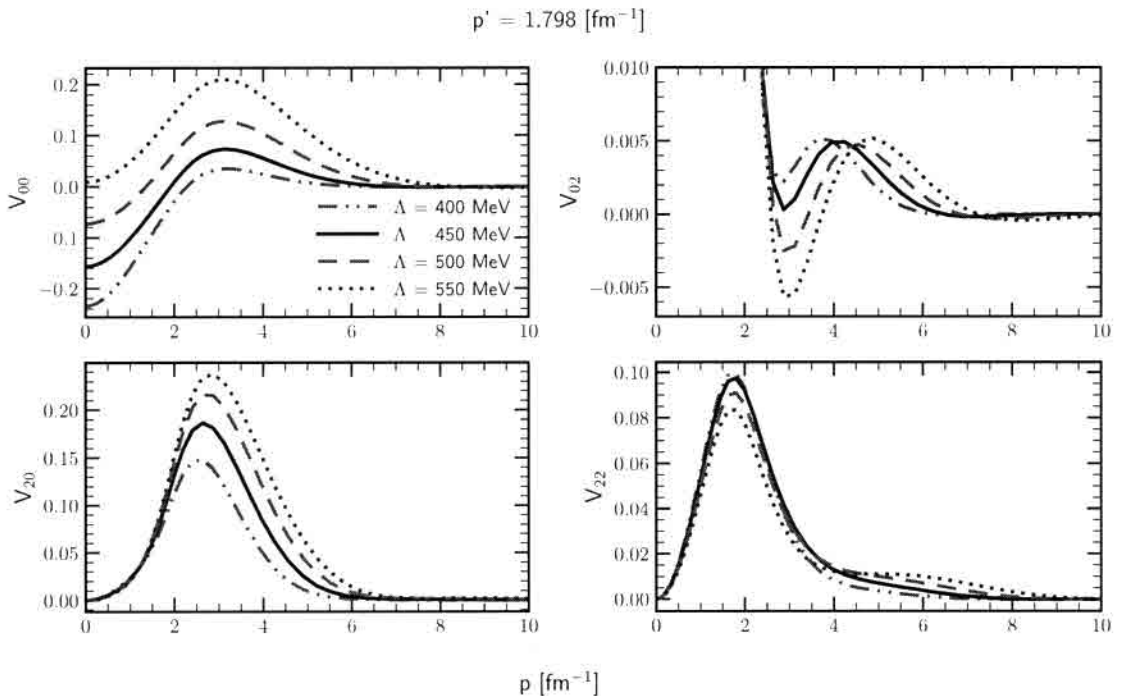


Figure 1.2: Matrix elements $\langle p|V|p'\rangle$ of the potential in coupled partial waves ${}^3S_1 - {}^3D_1$ as a function on the momentum p with fixed value of the momentum $p' = 1.798 \text{ fm}^{-1}$. Potential element $V_{ll'}$ is taken between two states with angular momenta l and l' where $l = 0$ stands for 3S_1 state and $l = 2$ for 3D_1 .

consistently from the same underlying theory of nuclear phenomena. I work with the SMS chiral interaction, and for that force the complete consistent MEC has not been derived yet. Consistency includes here also the same regularization as used for the iteration. While the derivation of such is ongoing [H. Krebs, private communication], at the moment only SNC is well established. Thus to mimic effects of the MEC, I apply the Siegert theorem [13, 14]. In general, this theorem allows to substitute explicit MEC terms by the $O(1/\hbar)$ component of the nuclear current (the charge density). It is less sensitive to MEC contributions (compared to spatial components of j_μ) and thus in its case the SNC approximation is sufficient. I use here the formulation of the Siegert theorem given in [14].

A more detailed discussion of electromagnetic currents used here is given in the Section 2.6.

time

(maybe better)

this should be zero

currents

make

iteration

* In case of ^3He or ^3H photodisintegration analogous matrix element $\langle \Psi_{final} | J^\mu | \Psi_{initial} \rangle$ have to be found, but now $|\Psi_{initial}\rangle$ is either ^3He or ^3H bound state and $\langle \Psi_{final} |$ describes or ^3N scattering state with all three nucleons unbound ~~in the~~ after reaction or N^2 scattering state with pair nucleon-deuteron in the final state.

CHAPTER 2

FORMALISM & NUMERICAL METHODS

I feel such explanation is necessary since later we are introducing ^3N and N^2 states without explanations. What they mean.

Despite the fact that the deuteron problem was solved long time ago, I will describe it briefly in order to introduce the notation and formalism. With that, for more complex ^3N case only slight extension will be needed.

In order to calculate any observable for the deuteron photodisintegration, one has to find a nuclear matrix elements:

$$N^\mu = \langle \Psi_{final} | J^\mu | \Psi_{initial} \rangle, \quad (2.1)$$

with two-nucleon wave function of the initial state $\Psi_{initial}$ ~~including two and three nucleon interaction~~, $\Psi_{initial} = \Psi_{deuteron}$; two-nucleon wave function of the final scattering state Ψ_{final} and a four-vector current operator J^μ which acts between initial and final two-nucleon states. In following I describe how to get ~~that~~ ^{these} quantities.

2.1 Deuteron bound state 2N bound state

^{to be consistent with other titles}

Let's find a deuteron bound state wave function $|\phi_d\rangle$. The time-independent Schrödinger equation for two particles expresses as:

$$(H_0 + V) |\phi_d\rangle = E_d |\phi_d\rangle, \quad (2.2)$$

with a kinetic energy H_0 and potential V . The kinetic energy H_0 can be represented in terms of relative and total momenta of the particles:

$$H_0 = \frac{\vec{p}_1^2}{2m_1} + \frac{\vec{p}_2^2}{2m_2} = \frac{\vec{p}^2}{2\mu} + \frac{\vec{P}^2}{2M}, \quad (2.3)$$

where the relative and total momenta are defined as follows:

$$\vec{p} = \frac{(m_1 \vec{p}_1 - m_2 \vec{p}_2)}{m_1 + m_2}, \quad (2.4)$$

$$\vec{P} = \vec{p}_1 + \vec{p}_2, \quad (2.5)$$

where $M = m_1 + m_2$ is a total mass, $\mu = \frac{m_1 m_2}{M}$ is a reduced mass of two nucleons and \vec{p}_i is a momentum of i -th particle.

Potential V is assumed to depend on the relative degrees of freedom only, so Eq. (2.2) may be decomposed into two separated equations:

$$\frac{\vec{p}^2}{2\mu} \langle \vec{p} | \Psi_{int} \rangle + \langle \vec{p} | V | \Psi_{int} \rangle = (E_d - E) \langle \vec{p} | \Psi_{int} \rangle \quad (2.6)$$

$$\frac{\vec{P}^2}{2M} \langle \vec{P} | \Psi \rangle = E \langle \vec{P} | \Psi \rangle, \quad (2.7)$$

 with $\langle \vec{p}, \vec{P} | H_0 | \phi_d \rangle = \frac{\vec{p}^2}{2\mu} \langle \vec{p} | \Psi_{int} \rangle + \frac{\vec{P}^2}{2M} \langle \vec{P} | \Psi \rangle$. So Ψ is a component of total wave function, which reflects a deuteron as a single object with momentum \vec{P} while Ψ_{int} is an internal wave function describing interaction between nucleons. Basis state $|\vec{p}\rangle$ obeys a completeness equation:

$$\int d^3 \vec{p} |\vec{p}\rangle \langle \vec{p}| = 1. \quad (2.8)$$

Eq. (2.6) is basically the Schrödinger equation for a single particle with mass μ in potential V and Eq. (2.7) can be regarded as a Schrödinger equation for particle with mass M in a free motion. Assuming that deuteron is at rest ($E = 0$) we can stick to the Eq.(2.6) only. Using completeness relation (2.8) we get:

i.e. directly with \vec{p} vectors

$$\frac{\vec{p}^2}{2\mu} \langle \vec{p} | \Psi_{int} \rangle + \int d\vec{p}' \langle \vec{p} | V | \vec{p}' \rangle \langle \vec{p}' | \Psi_{int} \rangle = E_d \langle \vec{p} | \Psi_{int} \rangle \quad (2.9)$$

Working in 3 dimensional space is difficult, especially numerically, so I follow a standard path and introduce the partial-wave decomposed representation (PWD) of the momentum state, adding spin and isospin degrees of freedom in the following form:

$$|p\alpha\rangle \equiv |p(ls)jm_j\rangle |tm_t\rangle, \quad (2.10)$$

where quantum numbers l , s , j , t are orbital angular momentum, total spin, total angular momentum and total isospin respectively. m_j and m_t are total angular momentum and isospin projections, respectively.

States $|p(ls)jm_j\rangle$ can be further decomposed to the more basic states than it is in (2.10), separating spin part as

$$|p(ls)jm_j\rangle = \sum_{m_l} c(lsj; m_l, m_j - m_l, m_j) |plm_l\rangle |s m_j - m_l\rangle. \quad (2.11)$$

Spin(isospin) states can be further represented via single-nucleon spin(isospin) states:

$$|sm_s\rangle = \sum_{m_1} c(\frac{1}{2} \frac{1}{2} s; m_1, m_s - m_1, m_s) \left| \frac{1}{2} m_1 \right\rangle \left| \frac{1}{2} m_s - m_1 \right\rangle, \quad (2.12)$$

$$|tm_t\rangle = \sum_{\nu_1} c(\frac{1}{2} \frac{1}{2} t; \nu_1, m_t - \nu_1, m_t) \left| \frac{1}{2} \nu_1 \right\rangle \left| \frac{1}{2} m_t - \nu_1 \right\rangle. \quad (2.13)$$

In Eqs.(2.11) -(2.13), $c(\dots)$ are Clebsh-Gordon coefficients. Nucleons are spin $\frac{1}{2}$ particles, and we also treat proton and neutron as the same particle in different isospin states, using convention in which isospin $\nu_1 = \frac{1}{2}$ stands for proton and $\nu_1 = -\frac{1}{2}$ is for neutron.

The states $|plm_l\rangle$ from Eq.(2.11) are orthogonal

$$\langle p'l'm'_l | plm_l \rangle = \frac{\delta(p - p')}{p^2} \delta_{ll'} \delta_{m_l m'_l} \quad (2.14)$$

and satisfy the completeness relation:

$$\sum_{l=0}^{\infty} \sum_{m_l=-l}^l \int dp p^2 | plm_l \rangle \langle plm_l | = 1 \quad (2.15)$$

Projection of $\langle \vec{p}' |$ states to $| plm_l \rangle$ leads to

$$\langle \vec{p}' | plm_l \rangle = \frac{\delta(|\vec{p}'| - p)}{p^2} Y_{lm_l}(\hat{p}'), \quad (2.16)$$

where $Y_{lm_l}(\hat{p}')$ is a spherical harmonic and 'hat' denotes a unit vector \hat{X} in direction of \vec{X} . Thus for the momentum vector:

$$\vec{p} \equiv |\vec{p}| \hat{p} \equiv p \hat{p}. \quad (2.17)$$

Nucleons are fermions so exchanging them leads to antisymmetry of the wave function. In PWD it results in additional requirement on allowed quantum numbers which is:

$$(-1)^{l+s+t} = -1. \quad (2.18)$$

In general, nuclear NN force conserves spin, parity and charge so

$$\langle p'\alpha' | V | p\alpha \rangle = \delta_{jj'} \delta_{mm'} \delta_{tt'} \delta_{m_t m_{t'}} \delta_{ss'} V_{l'l}^{sjtm_t}(p', p) \quad (2.19)$$

which introduces restrictions for particular sets of quantum numbers and α' . Strong interaction allows for change of the orbital angular momenta $l = j \pm 1$, $l' = j' \pm 1$. The channels, in which $l \neq l'$ is allowed, are called coupled channels and for the deuteron bound state one can find only one such PWD state combination: two coupled channels which are commonly denoted as 3S_1 and 3D_1 (the naming stands for ${}^{2s+1}l_j$). They correspond to $l = 0$ and $l = 2$ respectively (with $s = j = 1$ and $t = m_t = 0$). We will denote wave functions for these channels as $\phi_l(p)$ with $l = 0, 2$, such that:

$$\phi_l(p) = \langle p(ls)jm_l | \langle tm_t | \Psi_{int} \rangle = \langle p(l1)1m_d | \langle 00 | \Psi_{int} \rangle ; l = 0, 2. \quad (2.20)$$

In that new basis Eq.(2.9) takes a form of two coupled equations:

$$\frac{\vec{p}^2}{2\mu} \phi_l(p) + \sum_{l'=0,2} \int dp' p'^2 \langle p(l1)1m_d | \langle 00 | V | 00 \rangle | p'(l'1)1m_d \rangle \phi_{l'}(p') = E_d \phi_l(p), \quad (2.21)$$

for $l = 0, 2$. In case one does not have a matrix elements for the potential $\langle plm_l | V | p'l'm'_l \rangle$ in analytical form, but only numerical values for some grid of points are given, there is still one complication in the Eq.(2.21) - integration, which has to be discretized. In order to get rid of the integral I use a Gaussian quadrature method of numerical integration [17]. It allows me to replace an integral by the weighted sum: $\int_a^b f(x) dx = \sum_{i=1}^N \omega_i f(x_i)$. In current work I used $N = 72$ points in the interval from 0 to 50 fm^{-1} . Using this method, Eq.(2.21) becomes

$$\frac{p_i^2}{2\mu} \phi_l(p_i) + \sum_{l'=0,2} \sum_{j=0}^{N_p} \omega_j p_j^2 \langle p_i(l1) 1m_d | \langle 00 | V | 00 \rangle | p_j(l'1) 1m_d \rangle \phi_{l'}(p_j) = E_d \phi_l(p_i). \quad (2.22)$$

In practical computations, the same grid points p_i and p_j are used in order to optimize computational time. I solve this equation as an eigenvalue problem $M\Psi = E_d\Psi$ and in that way find simultaneously wave function values in grid of p points and the binding energy E_d . The binding energy E_d calculated with potentials at different chiral orders is presented in Fig. 2.1.

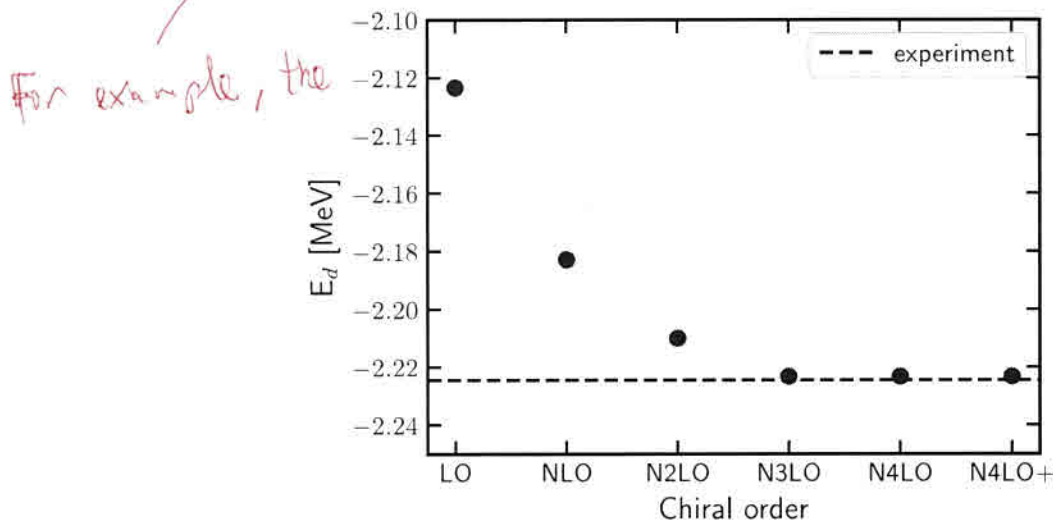


Figure 2.1: Deuteron binding energy calculated using the chiral SMS potential at different chiral orders as a mean value over all cutoffs. Experimental data is taken from [16].

An example of such wave functions is demonstrated in Fig. 2.2. The left panel demonstrates a wave function for $l = 0 - {}^3S_1$ while the right one - for $l = 2 - {}^3D_1$. Both plots consist of the curves for different cutoff values and using the chiral SMS potential at N^4LO^+ . The small deviation between lines show that cutoff dependence is rather weak at this stage and further discrepancies connected to the value of Λ may appear in other components of nuclear matrix elements.

2.2 2N scattering state

I work in the time-independent formulation of the scattering process. In such a case the Hamiltonian is:

$$H = H_0 + V, \quad (2.23)$$

where again H_0 is a kinetic energy operator, $H_0 = \frac{\vec{p}^2}{2m}$, and V is a nucleon-nucleon interaction. For a free particle motion, V will be absent and we will denote a corresponding energy eigenstate as a free particle state $|\vec{p}\rangle$. The scattering state $|\psi\rangle$ fulfills similar Schrödinger equation as $|\vec{p}\rangle$, with the same energy eigenvalue, but with the presence of the potential:

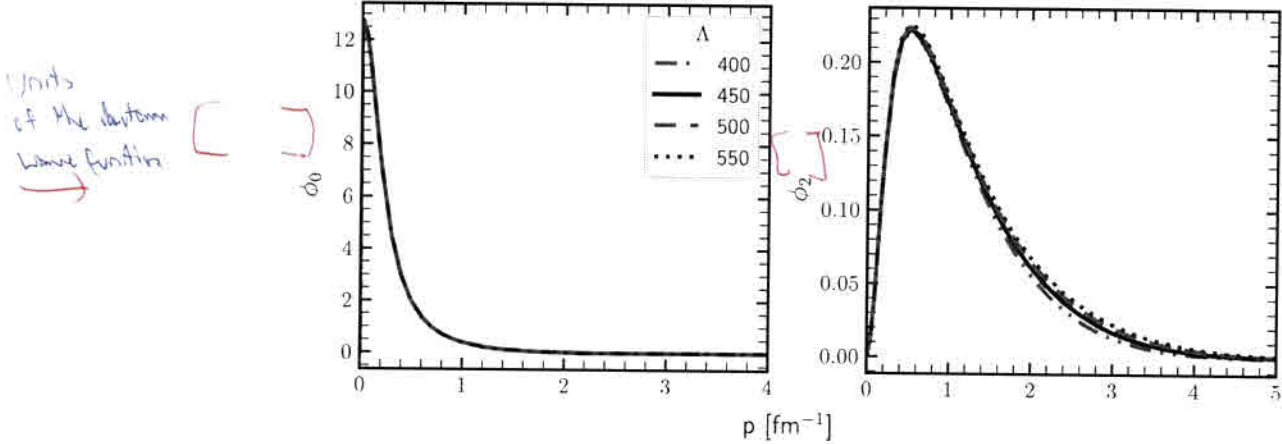


Figure 2.2: The deuteron wave function ϕ_l for $l=0$ (3S_1 partial wave)(left) and $l=2$ (3D_1) (right). Each curve shows results obtained with different values of the cutoff parameter Λ . The chiral SMS potential at $N^4\text{LO}^+$ was used.

$$\begin{cases} H_0 |\vec{p}\rangle &= E |\vec{p}\rangle, \\ (H_0 + V) |\psi\rangle &= E |\psi\rangle. \end{cases} \quad (2.24)$$

We are interested in solution for Eq. (2.24), so that $|\psi\rangle \rightarrow |\vec{p}\rangle$ as $V \rightarrow 0$ and both $|\psi\rangle$ and $|\vec{p}\rangle$ have the same energy eigenvalues E . As we have scattering process, the energy spectra for both operators H_0 and $H_0 + V$ are continuous.

From Eq. (2.24) it follows that

$$|\psi\rangle = \frac{1}{E - H_0} V |\psi\rangle + |\vec{p}\rangle, \quad (2.25)$$

which guarantees that application of the operator $(E - H_0)$ to the Eq. (2.25) results in the second equation from the set (2.24).

In order to deal with a singular operator $\frac{1}{E - H_0}$ in Eq. (2.25), the well-known technique is used to make such an operator complex by adding small imaginary number to the denominator so Eq. (2.25) becomes

$$|\psi\rangle = G_0(E \pm i\epsilon) V |\psi\rangle + |\vec{p}\rangle, \quad (2.26)$$

where G_0 is a free propagator:

$$G_0(z) = \frac{1}{z - H_0}. \quad (2.27)$$

Solution with $G_0(E - i\epsilon)$ corresponds to the incoming spherical wave, while $G_0(E + i\epsilon)$ - to the outgoing one. Since we are interested in the final scattering state, only the (+) sign survives.

Eq. (2.26) is known as the Lippmann-Schwinger equation (LSE). Defining the transition operator t :

$$t |\vec{p}\rangle = V |\psi\rangle \quad (2.28)$$

we can rewrite it as

$$|\psi\rangle = (1 + G_0(E + i\epsilon)t) |\vec{p}\rangle . \quad (2.29)$$

With substitution of Eq. (2.26) into Eq. (2.28) we can find an explicit form of the t operator:

$$\begin{aligned} t |\vec{p}\rangle &= VG_0(E + i\epsilon)V |\psi\rangle + V |\vec{p}\rangle = \\ &= VG_0(E + i\epsilon)t |\vec{p}\rangle + V |\vec{p}\rangle \end{aligned} \quad (2.30)$$

Getting rid off the initial state $|\vec{p}\rangle$ in the Eq. (2.30) we can get the LSE for the transition operator in the iterative form:

\nwarrow operator

$$\begin{aligned} t &= V + VG_0t = \\ &= V + VG_0V + VG_0VG_0V + \dots, \end{aligned} \quad (2.31)$$

which constitutes an infinite series of subsequent NN interactions and free propagators of nucleons.

In the partial-wave representation, the LSE Eq. (2.30) expresses as:

$$\begin{aligned} \langle p'(l's')j'm_{j'}| \langle t'm_{t'}|t(E)|tm_t\rangle |p(ls)jm_j\rangle &= \langle p'(l's')j'm_{j'}| \langle t'm_{t'}|V|tm_t\rangle |p(ls)jm_j\rangle + \\ &+ \sum_{\alpha''} \int_0^\infty dp'' p''^2 \langle p'(l's')j'm_{j'}| \langle t'm_{t'}|V|t''m_{t''}\rangle |p''(l''s'')j''m_{j''}\rangle \\ &\times \frac{1}{E + i\epsilon - p''^2/m} \langle p''(l''s'')j''m_{j''}| \langle t''m_{t''}|t(E)|tm_t\rangle |p(ls)jm_j\rangle , \end{aligned} \quad (2.32)$$

which after using symmetries of potential matrix elements (2.19) reduces to

$$\begin{aligned} \langle p'(l's')jt|t(E)|p(ls)jt\rangle &= \langle p'(l's)jt|V|p(ls)jt\rangle + \\ &+ \sum_{\alpha''} \int_0^\infty dp'' p''^2 \langle p'(l's)jt|V|p''(l''s)jt\rangle \\ &\times \frac{1}{E + i\epsilon - p''^2/m} \langle p''(l''s)jt|t(E)|p(ls)jt\rangle . \end{aligned} \quad (2.33)$$

I solve Eq. (2.33) numerically, which again requires discretisation and therefore leads to set of linear equations. Finally, using Eq. (2.29) and denoting the momentum state of two nucleons with spin projections m_p and m_n as $\langle \phi m_p m_n |$, we can write Eq. (2.1) as

\rightarrow

$$N^\mu = \langle \phi m_p m_n | (1 + G_0(E + i\epsilon)t) J^\mu | \Psi_{\text{deuteron}} \rangle \quad (2.34)$$

2.3 3N bound state

The 3N bound state is described by the Schrödinger equation for 3N system, ~~ie~~ including two- and three- nucleon interaction, and ~~its~~ total wave function obeys the following equation:

with Hamiltonian comprising
of ~~the~~
 $\langle \Psi |$ $\Psi \rangle$
The bound state

$$|\Psi\rangle = G_0(E + i\epsilon) \sum_{j=1}^3 (V_j + V_4^j) |\Psi\rangle, \quad (2.35)$$

where G_0 is a 3N free propagator as in Eq. (2.27), V_j - is a two-body potential acting between nucleons k and l (j, k and l - numerate nucleons, $j, k, l \in \{1, 2, 3\}$ and $j \neq k \neq l$), V_4^j is a component of three-body potential $V_4 = \sum_{j=1}^3 V_4^j$ symmetrical under exchange of nucleons k and l , and E - is a 3N binding energy.

Eq. (2.35) can be split into three independent equations for so-called Faddeev components $|\psi_j\rangle$

$$|\Psi\rangle = \sum_{j=1}^3 |\psi_j\rangle. \quad (2.36)$$

which fulfills separately

$$|\psi_j\rangle = G_0(E + i\epsilon)(V_j + V_4^j) |\Psi\rangle. \quad (2.37)$$

Next, I introduce a permutation operator P , which is a combination of operators P_{jk} :

$$P = P_{12}P_{23} + P_{13}P_{32}. \quad (2.38)$$

The operator ~~component~~ P_{jk} acting on the state interchange the momenta and quantum numbers of the nucleons j and k .

Using definitions (2.38) and (2.36), one can rewrite Eq. (2.37) as:

$$|\psi_j\rangle = G_0(E + i\epsilon)t_j P |\psi_j\rangle + (1 + G_0(E + i\epsilon)t_j)G_0(E + i\epsilon)V_4^j(1 + P) |\psi_j\rangle, \quad (2.39)$$

where t_j is a two-body t-operator which obeys Eq. (2.30) for corresponding two-body potential V_j . I solve Eq. (2.39) numerically to find $|\psi_j\rangle$ and the binding energy E . To do that, I perform PWD again.

The partial wave representation of the Eq. (2.39) is obtained using following 3N states:

$$|p, q, \alpha_{J, M_J}\rangle = \left| p, q, (ls)j, (\lambda, \frac{1}{2})I(jI)JM; (t, \frac{1}{2})TM_T \right\rangle_1, \quad (2.40)$$

where index 1 states the choice of the Jacobi momenta, such that p is a relative momentum of the nucleons 2 and 3. Values l, s and j are quantum numbers in the two-body subsystem consisted of nucleons 2 and 3. λ is the orbital angular momentum with respect to the c.m. of the particles 2 and 3, of the first particle which spin is $\frac{1}{2}$ and I is its total angular momentum. J and M_J are the total angular momentum of the 3N system and its projection on the z-axis respectively. t is a total isospin of the 2-3 subsystem whereas T and M_T are the total isospin of the 3N system and its projection on the z-axis, respectively.

The Jacobi momenta \vec{p} and \vec{q} are defined as: $\vec{p} = \vec{p}_1 + \vec{p}_2$ and $\vec{q} = \vec{p}_1 + \vec{p}_3$

*give equations
from Hahn book*

2.4 3N scattering state

Let us introduce an asymptotic state $|\Phi_j^{3N}\rangle$ describing a free motion of three nucleons j, k, l with particles k and l having relative momentum \vec{p} and particle j moving with

with respect
momentum \vec{q} relatively to the center of mass $(k - l)$ *of system*:

$$|\Phi_j^{3N}\rangle \equiv \frac{1}{\sqrt{2}}(1 - P_{kl})|\vec{p}(kl)\vec{q}(j)\rangle. \quad (2.41)$$

The Jacobi momenta \vec{p} and \vec{q} build the total energy of three nucleons in the 3N-c.m. system:

$$E_{3N} = \frac{|\vec{p}|^2}{m} + \frac{3|\vec{q}|^2}{4m}. \quad (2.42)$$

Using a free propagator $G(E_{3N} - i\epsilon)$ we can come up with the total 3N scattering state

$$|\Psi^{(-)}\rangle^{3N} = \frac{1}{\sqrt{3}} \sum_j |\Psi_j^{(-)}\rangle^{3N}, \quad (2.43)$$

where auxiliary scattering states $|\Psi_j^{(-)}\rangle^{3N}$ are defined as [17]

$$|\Psi_j^{(-)}\rangle^{3N} \equiv \lim_{\epsilon \rightarrow 0} i\epsilon G(E_{3N} - i\epsilon) |\Phi_j^{3N}\rangle. \quad (2.44)$$

The state $|\Psi_j^{(-)}\rangle^{3N}$ together with the state $|\Phi_j^{3N}\rangle$ fulfills an equation [17]

$$|\Psi_j^{(-)}\rangle^{3N} = |\Phi_j^{3N}\rangle + G_0(V_1 + V_2 + V_3 + V_4)|\Psi_j^{(-)}\rangle^{3N}. \quad (2.45)$$

Defining the antisymmetrized Faddeev components, and using index "i" instead of "j"

$$|F_i^0\rangle \equiv G_0(V_i + V_4)(1 + P)|\Psi_i^{(-)}\rangle^{3N} \quad (2.46)$$

we obtain a 3N scattering wave function as:

$$\begin{aligned} |\Psi^{(-)}\rangle^{3N} &= \frac{1}{\sqrt{3}} \left(\sum_{i=1}^3 |\Phi_i^{3N}\rangle + G_0(V_1 + V_2 + V_3 + V_4) \sum_{i=1}^3 |\Psi_i^{(-)}\rangle^{3N} \right) \\ &= \frac{1}{\sqrt{3}} \left(\sum_{i=1}^3 |\Phi_i^{3N}\rangle + \sum_{i=1}^3 |F_i^0\rangle \right) = \frac{1}{\sqrt{3}}(1 + P)(|\Phi_1^{3N}\rangle + |F_1^0\rangle). \end{aligned} \quad (2.47)$$

In this case the nuclear matrix element $N_\mu^{3N} = \langle \Psi^- | j^\mu | \psi_i \rangle$ (with $|\psi_i\rangle$ being the Faddeev component of the 3N bound state (2.36)) is [18, 19] ???

$$\begin{aligned} N_\mu^{3N} &= \frac{1}{\sqrt{3}} \langle \Phi_1^{3N} | (1 + P) j_\mu | \Psi_i \rangle + \frac{1}{\sqrt{3}} \langle \Phi_1^{3N} | t_1^+ G_0^+ (1 + P) j_\mu | \Psi_i \rangle \\ &\quad + \frac{1}{\sqrt{3}} \langle \Phi_1^{3N} | t_1^+ G_0^+ P | U_\mu \rangle + \frac{1}{\sqrt{3}} \langle \Phi_1^{3N} | P | U_\mu \rangle, \end{aligned} \quad (2.48)$$

where U_μ fulfills the following equation:

I meant here one
more reference
Shibinshi et al. Eur. Phys. J. A24 (2005) 31
Recent formulations...)

$$|U_\mu\rangle = \left[t_1^+ G_0^+ + \frac{1}{2}(1+P)V_4^{(1)}G_0^+ (1+t_1^+ G_0^+) \right] (1+P)j_\mu |\Psi_i\rangle \\ + \left[t_1^+ G_0^+ P + \frac{1}{2}(1+P)V_4^{(1)}G_0^+ (1+t_1^+ G_0^+) P \right] |U_\mu\rangle. \quad (2.49)$$

Eq. (2.49) is being solved numerically in PWD. The techniques applied closely resemble those presented in [48] for N-d elastic scattering. *are the same as scheme.*

2.5 Nd scattering state

Analogously to the bound state, one can express a nucleon-deuteron scattering state using a permutation operator Eq. (2.38).

$$|\Psi^{(-)}\rangle^{Nd} = \frac{1}{\sqrt{3}} \sum_j |\Psi_j^{(-)}\rangle^{Nd} \quad (2.50)$$

Further a scattering state $|\Psi_j^{(-)}\rangle^{Nd}$ can be expressed in terms of asymptotic state $|\Phi_j^{Nd}\rangle$, in which particles k and l form a deuteron and the third particle (nucleon j) propagates freely with a relative momentum \vec{q}_0 with respect to the deuteron:

$$|\Psi_j^{(-)}\rangle^{Nd} \equiv \lim_{\epsilon \rightarrow 0} i\epsilon G(E_{Nd} - i\epsilon) |\Phi_j^{Nd}\rangle \quad (2.51)$$

$$|\Phi_j^{Nd}\rangle \equiv |\Phi_{d(k,l)}\rangle |\vec{q}_0\rangle, \quad (2.52)$$

where $|\Phi_{d(k,l)}\rangle$ is a deuteron wave function and $|\vec{q}_0\rangle$ - a free particle state and $G(t)$ is a free propagator of N-d pair. E_{Nd} is a total energy of the N-d system:

$$E_{Nd} = E_d + \frac{3|\vec{q}_0|^2}{4m}, \quad (2.53)$$

where E_d is the deuteron binding energy and m denotes the nucleon mass.

$|\Psi^{(-)}\rangle^{Nd}$ can be expressed by the Faddeev components

$$|\Psi^{(-)}\rangle^{Nd} = \frac{1}{\sqrt{3}} (1+P) |F_1\rangle, \quad (2.54)$$

where

$$|F_1\rangle = |\phi_1^{Nd}\rangle G_0(\nu_1 + \nu_2 + \nu_3 + \nu_4) \sum_{j=1}^3 |\Psi_j^{(-)}\rangle^{Nd}. \quad (2.55)$$

The nuclear matrix element $N_\mu^{Nd} = \langle \Psi^- | j_\mu | \Psi_i \rangle$ (with Ψ_i - bound state) is now [48, 49] *???*

$$N_\mu^{Nd} = \frac{1}{\sqrt{3}} \langle \Phi_1^{Nd} | (1+P) j_\mu | \Psi_i \rangle + \frac{1}{\sqrt{3}} \langle \Phi_1^{Nd} | P | U_\mu \rangle \quad (2.56)$$

with U_μ being a solution to *of Eq (2.49)*. *Fact that solving*

one Eq (2.49) opens opportunity to compute both

N_μ^{Nd} and N_μ^{3N} is a great advantage of the presented formulation

* Each j_μ^n describes interaction of photon with all relevant permutations of n nucleons, i.e. j_μ^n is ...

CHAPTER 2. FORMALISM & NUMERICAL METHODS

$$\begin{aligned} |U_\mu\rangle = & \left[t_1^+ G_0^+ + \frac{1}{2}(1+P)V_4^{(1)}G_0^+ (1+t_1^+ G_0^+) \right] (1+P)j_\mu |\Psi_i\rangle + \\ & + \left[t_1^+ G_0^+ P + \frac{1}{2}(1+P)V_4^{(1)}G_0^+ (1+t_1^+ G_0^+) P \right] |U_\mu\rangle \end{aligned} \quad (2.57)$$

Eq. (2.57) is being solved numerically in a same way as Eq. (2.49), namely applying PWD as it is described in [18].

2.6 Nuclear electromagnetic current

The electromagnetic current operator for 2N (3N) system is constructed from the one- and many-body currents:

$$j_\mu = j_\mu^1 + j_\mu^2 (+j_\mu^3). \quad (2.58)$$

In Eq. (2.58) j_μ^n is a contribution from the interaction between photon and n nucleons (j_μ^3 is presented in 3N system only), and (j_μ^1) is a sum of interactions with each nucleon in the system separately. of

In case of the Regarding the photodisintegration process, only a single nucleon current (1NC) is used, so I stick to its definition here. In the Hamiltonian framework, the nucleons are constrained to lie on the mass shell. The general current expression for a single nucleon at the spacetime point zero, denoted as $j_\mu^1(0)$, is computed between the initial nucleon momentum $p \equiv (p_0 = \sqrt{M_N^2 + \vec{p}^2}, \vec{p})$ and the final momentum $p' \equiv (p'_0 = \sqrt{M_N^2 + \vec{p}'^2}, \vec{p}')$. This computation yields the following expression: matrix elements:

$$\begin{aligned} \langle \vec{p}' | j_\mu^1(0) | \vec{p} \rangle = & \bar{u}(\vec{p}' s') (\gamma^\mu F_1 + i\sigma^{\mu\nu} (p' - p)_\nu F_2) u(\vec{p} s) \\ = & \bar{u}(\vec{p}' s') (G_M \gamma^\mu - F_2 (p' + p)^\mu) u(\vec{p} s). \end{aligned} \quad (2.59)$$

In the above equation, ie. including two- and three-nucleon interaction, the symbols $u(\vec{p} s)$ represent Dirac spinors for particle having momentum \vec{p} and spin s , F_1 and F_2 are the Dirac and Pauli form factors of the nucleon, respectively, and $G_M \equiv F_1 + 2M_N F_2$ denotes the magnetic form factor of the nucleon. The proton charge e is extracted from the matrix element. In this thesis, only the nonrelativistic limit of Eq. (2.59) is considered, which leads to well-known expressions for the operators for the current: [folk report]

$$\langle \vec{p}' | j_0^1 | \vec{p} \rangle = (G_E^p \Pi^p + G_E^n \Pi^n), \quad (2.60)$$

$$\langle \vec{p} | j_1^1 | \vec{p} \rangle = \frac{\vec{p} + \vec{p}'}{2M_N} (G_E^p \Pi^p + G_E^n \Pi^n) + \frac{i}{2M_N} (G_M^p \Pi^p + G_M^n \Pi^n) \vec{\sigma} \times (\vec{p}' - \vec{p}). \quad (2.61)$$

The electric form factor, denoted as G_E , is defined as, $G_E \equiv F_1 + \frac{(p' - p)^2}{2M_N} F_2$ and represents the neutron (n) and proton (p) form factors. Both electric and magnetic form factors, G_E and G_M , are normalized as:

$$\approx G_E(Q^2) \approx G_M(Q^2)$$

* with the latter one constrained by the four-momentum transfer Q from photon to nucleon.

no arguments w/ E_E and E_M

$$G_E^n(0) = 0$$

$$G_E^p(0) = 1$$

$$G_M^n(0) = -1.913$$

$$G_M^p(0) = 2.793$$

*but at low energies
the usual here
will make leads to
practically same values
(2.62)
of the form factors*

The above values correspond to nucleons with point-like characteristics. While all the form factors depend on the squared four-momentum transfer $(p' - p)^2$, in the nonrelativistic regime, it is common to use the squared three-momentum transfer $-(\vec{p}' - \vec{p})^2$ or even set it to zero for interactions involving real photons. Numerous authors have investigated the properties of electromagnetic nucleon form factors through theoretical and experimental approaches, as discussed in [50, 51]. Π^p (Π^n) in Eq. (2.61) is a proton (neutron) isospin projection operator.

The two-nucleon current contribution is in that work taken into account via Siegert approach [13, 11, 52]. In order to do that we break down the single nucleon current matrix elements into multipole components and represent some of the electric multipoles using the Coulomb multipoles, which arise from the single nucleon charge density operator [53]. This is acceptable because, in low-energy situations, contributions from many nucleons to the nuclear charge density are typically insignificant. We then obtain the rest of the electric multipoles and all of the magnetic multipoles exclusively from the single nucleon current operators.

In 3N system we have following components of the 1NC:

expressions for

$$(j_\mu^1)^\pm \equiv j_{\mu}^{1,\text{conv}} + j_{\mu}^{1,\text{spin}}$$

$$\langle \vec{p}', \vec{q}' | j_0^1 | \vec{p}, \vec{q} \rangle = \int d\vec{p}'' d\vec{q}'' \left\langle \vec{p}', \vec{q}' \left| \frac{1}{2} (1 + \tau(1)_z) F_1^p + \frac{1}{2} (1 - \tau(1)_z) F_1^n \right| \vec{p}'', \vec{q}'' \right\rangle \\ \left\langle \vec{p}'', \vec{q}'' - \frac{2}{3} \vec{Q} \right| \vec{p}, \vec{q} \rangle \quad (2.63)$$

$$\langle \vec{p}', \vec{q}' | j_{\pm}^{1,\text{conv}} | \vec{p}, \vec{q} \rangle = \frac{1}{m} \int d\vec{p}'' d\vec{q}'' \langle \vec{p}', \vec{q}' | \left[\frac{1}{2} (1 + \tau(1)_z) F_1^p + \frac{1}{2} (1 - \tau(1)_z) F_1^n \right] q_{\pm} \\ \langle \vec{p}'', \vec{q}'' \rangle \left\langle \vec{p}'', \vec{q}'' - \frac{2}{3} \vec{Q} \right| \vec{p}, \vec{q} \rangle \quad (2.64)$$

$$\langle \vec{p}', \vec{q}' | j_{\pm}^{1,\text{spin}} | \vec{p}, \vec{q} \rangle = \frac{i}{2m} \int d\vec{p}'' d\vec{q}'' \langle \vec{p}', \vec{q}' | * \left[\frac{1}{2} (1 + \tau(1)_z) (F_1^p + 2mF_2^p) + \frac{1}{2} (1 - \tau(1)_z) (F_1^n + 2mF_2^n) \right] \\ * (\vec{\sigma}(1) \times \vec{Q})_{\pm} \langle \vec{p}'', \vec{q}'' \rangle \left\langle \vec{p}'', \vec{q}'' - \frac{2}{3} \vec{Q} \right| \vec{p}, \vec{q} \rangle. \quad (2.65)$$

convention

In Eq. (2.64) and Eq. (2.65) we present a conventional and spin currents which combined form a spatial component of the single nucleon current $j_{\pm}(0)$. Here I use a model of M. Garu and W. Krümpelmann [53] for which:

In my thesis

$$F_1^p(0) = 1 \quad 2mF_2^p(0) = 1.793 \quad (2.66)$$

$$F_1^n(0) = 0 \quad 2mF_2^n(0) = -1.913. \quad (2.67)$$

2.7 Pion absorption

For the pion absorption I include explicitly two nucleon current (2NC) as well as 1NC. Thus the absorption operator $\rho = \rho(1) + \rho(1, 2)$, where absorption on a single nucleon is included in $\rho(1)$ and $\rho(1, 2)$ plays a role of two-body charge current. The matrix element of the single nucleon pion absorption operator $\rho(1)$ in momentum-space for nucleon 1 relies on the nucleon's incoming momentum (\mathbf{p}) and outgoing momentum (\mathbf{p}'):

$$\langle \mathbf{p}' | \rho(1) | \mathbf{p} \rangle = -\frac{g_A M_\pi}{\sqrt{2} F_\pi} \frac{(\mathbf{p}' + \mathbf{p}) \cdot \boldsymbol{\sigma}_1}{2M} (\tau_1)_-, \quad (2.68)$$

where the values of the nucleon axial vector coupling, pion decay constant, and negative pion mass are $g_A = 1.29$, $F_\pi = 92.4$ MeV, and $M_\pi = 139.57 \frac{\text{MeV}}{c^2}$, respectively. $\rho(1)$ operates in the spin and isospin spaces and involves the Pauli spin (isospin) operator $\boldsymbol{\sigma}_1$ (τ_1) for nucleon 1 and the isospin lowering operator $(\tau_1)_- \equiv ((\tau_1)_x - i(\tau_1)_y)/2$. As before we use the average "nucleon mass" $M \equiv \frac{1}{2}(M_p + M_n)$ where the proton mass is M_p and neutron mass is M_n .

The 2N part of ρ at LO has the form [57]

$$\langle \mathbf{p}'_1 \mathbf{p}'_2 | \rho(1, 2) | \mathbf{p}_1 \mathbf{p}_2 \rangle = (v(k_2) \mathbf{k}_2 \cdot \boldsymbol{\sigma}_2 - v(k_1) \mathbf{k}_1 \cdot \boldsymbol{\sigma}_1) \times \frac{i}{\sqrt{2}} [(\tau_1) \times (\tau_2)]_x - i[(\tau_1) \times (\tau_2)]_y,$$

where $\mathbf{k}_1 = \mathbf{p}'_1 - \mathbf{p}_1$, $\mathbf{k}_2 = \mathbf{p}'_2 - \mathbf{p}_2$ and the formfactor $v(k)$ reads

$$v(k) = \frac{1}{(2\pi)^3} \frac{g_A M_\pi}{4F_\pi^3} \frac{1}{M_\pi^2 + k^2}. \quad (2.70)$$

In case of the pion absorption process we follow a standard procedure including partial wave states for both 2N and 3N induced nucleus. For 2N this is $\langle \mathbf{p} + \frac{1}{2}\mathbf{P}_f | \rho(1) | \mathbf{p} - \frac{1}{2}\mathbf{P}_f + \mathbf{P}_i \rangle$ while for 3N case $\langle \mathbf{q} + \frac{1}{3}\mathbf{P}_f | \rho(1) | \mathbf{q} - \frac{2}{3}\mathbf{P}_f + \mathbf{P}_i \rangle$.

For the $\pi^- + {}^2\text{H} \rightarrow n + n$ reaction, the nuclear matrix element for the transition operator is given by:

$$N_{nn}(m_1, m_2, m_d) = {}^{(-)} \langle \mathbf{p}_0 | m_1 m_2 | \mathbf{P}_f \rangle = 0 | \rho | \phi_d m_d | \mathbf{P}_i \rangle = 0, \quad (2.71)$$

where $| \mathbf{p}_0 m_1 m_2 | \mathbf{P}_f \rangle = 0 \rangle^{(-)}$ denotes the 2N scattering state [56].

The total absorption rate for this reaction would be: ~~expresses a~~ reaction prob

$$\Gamma_{nn} = \frac{(\alpha M'_d)^3 c M_n p_0}{2M_{\pi^-}} \int d\hat{\mathbf{p}}_0 \frac{1}{3} \sum_{m_1, m_2, m_d} | N_{nn}(m_1, m_2, m_d) |^2. \quad (2.72)$$

Turning to 3N system I investigate pion absorption in ${}^3\text{He}$ or ${}^3\text{H}$ with various final states. For $\pi^- + {}^3\text{He} \rightarrow n + d$ reaction the most important step in obtaining predictions is calculating the matrix element of the 3N transition operator ρ_{3N} , which is the ρ acting between the initial ${}^3\text{He}$ and the final ${}^3\text{N}$ scattering state immersed in 3N space:

Nd

$$N_{nd}(m_n, m_d, m_{^3\text{He}}) \equiv {}^{(-)} \langle \Psi_{nd} | m_n m_d | \mathbf{P}_f = 0 | \rho_{3N} | \Psi_{^3\text{He}} m_{^3\text{He}} | \mathbf{P}_i = 0 \rangle. \quad (2.73)$$

Given Eq. (2.73) the total absorption rate may be obtained from the following:

$$\Gamma_{nd} = \mathcal{R} \frac{16 (\alpha^3 M'_{^3\text{He}})^3 c M q_0}{9 M_{\pi^-}} \int d\hat{\mathbf{q}}_0 \frac{1}{2} \sum_{m_n, m_d, m_{^3\text{He}}} |N_{nd}(m_n, m_d, m_{^3\text{He}})|^2, \quad (2.74)$$

where $M'_{^3\text{He}} = \frac{M_{^3\text{He}} M_{\pi^-}}{M_{^3\text{He}} + M_{\pi^-}}$ is now the reduced mass of the $\pi^- - {}^3\text{He}$ system. The factor $\mathcal{R} = 0.98$ appears due to the finite volume of the ${}^3\text{He}$ charge [57]. The final state energy is expressed in terms of the neutron momentum (\mathbf{q}_0)

$$M_\pi + M_{^3\text{He}} \approx M_n + M_d + \frac{3}{4} \frac{\mathbf{q}_0^2}{M}, \quad (2.75)$$

The full 3N breakup is calculated in a similar way and the total absorption rate for $\pi^- + {}^3\text{He} \rightarrow p + n + n$ reaction is defined as follows

$$\begin{aligned} \Gamma_{pnn} = & \mathcal{R} \frac{16 (\alpha M'_{^3\text{He}})^3 c M}{9 M_{\pi^-}} \int d\hat{\mathbf{q}} \int_0^{2\pi} d\phi_p \int_0^\pi d\theta_p \sin \theta_p \\ & \times \int_0^{p_{max}} dp p^2 \sqrt{\frac{4}{3} (ME_{pq} - p^2)} \frac{1}{2} \sum_{m_1, m_2, m_3, m_{^3\text{He}}} |N_{pnn}(m_1, m_2, m_3, m_{^3\text{He}})|^2 \end{aligned} \quad (2.76)$$

with

$$N_{pnn}(m_1, m_2, m_3, m_{^3\text{He}}) \equiv {}^{(-)} \langle \Psi_{pnn} | m_1 m_2 m_3 | \mathbf{P}_f = 0 | \rho_{3N} | \Psi_{^3\text{He}} m_{^3\text{He}} | \mathbf{P}_i = 0 \rangle \quad (2.77)$$

E_{pq} is the internal energy of the final 3N state and can be expressed in terms of the Jacobi relative momenta (\mathbf{p}) and (\mathbf{q})

$$M_\pi + M_{^3\text{He}} \approx 3M + \frac{\mathbf{p}^2}{M} + \frac{3}{4} \frac{\mathbf{q}^2}{M} \equiv 3M + E_{pq} = 3M + \frac{p_{max}^2}{M} = 3M + \frac{3}{4} \frac{q_{max}^2}{M}. \quad (2.78)$$

In Eq. (2.78) p_{max} and q_{max} are maximal kinematically allowed values of Jacobi momenta p and q , respectively.

Analogously, the total absorption rate for $\pi^- + {}^3\text{H} \rightarrow n + n + n$ reads

$$\begin{aligned} \Gamma_{nnn} = & \frac{2 (\alpha M'_{^3\text{H}})^3 c M}{27 M_{\pi^-}} \int d\hat{\mathbf{q}} \int_0^{2\pi} d\phi_p \int_0^\pi d\theta_p \sin \theta_p \\ & \times \int_0^{p_{max}} dp p^2 \sqrt{\frac{4}{3} (ME_{pq} - p^2)} \frac{1}{2} \sum_{m_1, m_2, m_3, m_{^3\text{H}}} |N_{nnn}(m_1, m_2, m_3, m_{^3\text{H}})|^2 \end{aligned} \quad (2.79)$$

with

$$N_{nnn}(m_1, m_2, m_3, m_{^3\text{H}}) \equiv {}^{(-)} \langle \Psi_{nnn} | m_1 m_2 m_3 \mathbf{P}_f = 0 | \rho_{3N} | \Psi_{^3\text{H}} m_{^3\text{H}} \mathbf{P}_i = 0 \rangle \quad (2.80)$$

In the Results section I also demonstrate predictions of the differential absorption rates. The natural domain is that defined by energies of outgoing nucleons (E_1, E_2); in such a case the differential absorption rate $d^2\Gamma_{pnn}/(dE_1 dE_2)$ expresses as [56]

$$\frac{d^2\Gamma_{pnn}}{dE_1 dE_2} = \mathcal{R} \frac{64\pi^2 (\alpha M'_{^3\text{He}})^3 c M^3}{3M_{\pi^+}} \times \frac{1}{2} \sum_{m_1, m_2, m_3, m_{^3\text{He}}} |N_{pnn}(m_1, m_2, m_3, m_{^3\text{He}})|^2.$$

[56]
line

The kinematically allowed region is restricted to energies fulfilling the condition $-1 \leq \frac{E-2E_1-2E_2}{2\sqrt{E_1 E_2}} \leq 1$

One can also calculate differential absorption rate with respect to the dimensionless variables x and y which are frequently used in the literature, specifically to build so-called Dalitz plots [58]

$$\begin{aligned} x &= \sqrt{3}(E_1 + 2E_2 - E)/E, \\ y &= (3E_1 - E)/E. \end{aligned} \quad (2.82)$$

Such definition leads to simple kinematically allowed region, namely to the disk $r^2 \equiv x^2 + y^2 \leq 1$. One can evaluate $d^2\Gamma_{pnn}/(dx dy)$ or (using polar coordinates) $d^2\Gamma_{pnn}/(dr d\phi)$ and relate it with $\frac{d^2\Gamma_{pnn}}{dE_1 dE_2}$. The same can be done for $\frac{d^2\Gamma_{pnn}}{dE_1 d\phi}$ and $\frac{d^2\Gamma_{pnn}}{d\phi dy}$.

2.8 Theoretical uncertainties

Striving to achieve valuable theoretical results, we cannot omit the estimation of their uncertainty. There are various sources of predictions uncertainty. The three most important are: the truncation error, the cutoff dependence and the uncertainty related to various models of the nuclear interaction. The latter can be easily estimated by computing predictions arising from various models, see discussion below. The way how to estimate the first two types of uncertainties, together with a short discussion of remaining types of uncertainties are given below.

Sources of theoretical errors is

Truncation error

As it was mentioned above, each subsequent order of the chiral expansion provides us with more and more sophisticated potential which is expected to increase accuracy of data description. Starting from the leading order (LO) and coming next to N2LO, N3LO etc., we take into account more topologies (equivalents of Feynmann diagrams) and in result potential is expected to provide us with more precise predictions for the regarded process and observables. However, the chiral expansion (as any expansion) in principle can be continued up to the infinity, improving the resulting series. In practice we are limited to a finite, rather small, orders and we would like to find out the uncertainty

appearing from cutting off the remaining part of the expansion. That type of theoretical uncertainty is called a truncation error. Various methods to estimate its value have been proposed [59–63]. Typically predictions at lower orders serve as input information to get truncation error at given order. It is worth adding that Bayesian analysis is also used for truncation error estimation.

We use the method proposed in [61]. Let us regard some prediction $X^i(p)$ for observable X which is calculated at i -th order of the chiral expansion with the expansion parameter Q ($i = 0, 2, 3\dots$)¹. Here p specifies a momentum scale of the reaction. In the case of photodisintegration p is given by a photon's momentum.

If we define the difference between observables at each subsequent orders as:

$$\Delta X^{(2)} = |X^{(2)} - X^{(0)}|, \quad \Delta X^{(i>2)} = |X^{(i)} - X^{(i-1)}|, \quad (2.83)$$

then chiral expansion for X can be written as:

$$X = X^{(0)} + \Delta X^{(2)} + \Delta X^{(3)} + \dots + \Delta X^{(i)}. \quad (2.84)$$

The truncation error at i -th order, $\delta X^{(i)}$, is estimated using values of the observable obtained at lower orders as following:

$$\delta X^{(0)} = Q^2 |X^{(0)}|, \quad (2.85)$$

$$\delta X^{(i)} = \max_{2 \leq j \leq i} (Q^{i+1} |X^{(0)}|, Q^{i+1-j} |\Delta X^{(j)}|). \quad (2.86)$$

Additionally, following [61] I use the actual high-order predictions (if known) in order to specify uncertainties at lower orders, so that:

$$\delta X^{(i)} \geq \max_{j,k} (|X^{j \geq i} - X^{k \geq i}|) \quad (2.87)$$

and to be conservative I use additional restriction:

$$\delta X^{(i)} \geq Q \delta X^{(i-1)}. \quad (2.88)$$

All the conditions above assume that we use the whole available information at hand. In [61] it was shown that such method is equivalent to the Bayesian approach proposed there.

Cut-off dependence

Another theoretical uncertainty comes from the choice of the cutoff parameter's value or regulator described in the Chapter 1.

In the case of the SMS interaction its free parameters have been obtained from data for four values of the cutoff parameter Λ : 400, 450, 500 and 550 MeV [25]. Using each of these values, one obtains different predictions which, of course, can further differ from actual (experimental) value. Therefore the choice of Λ value may affect a quality of the prediction.

¹As mentioned in Sec. 1, we do not have a first order of expansion because this term in chiral expansion is always vanished and NLO corresponds to the quadratic term (number 2)

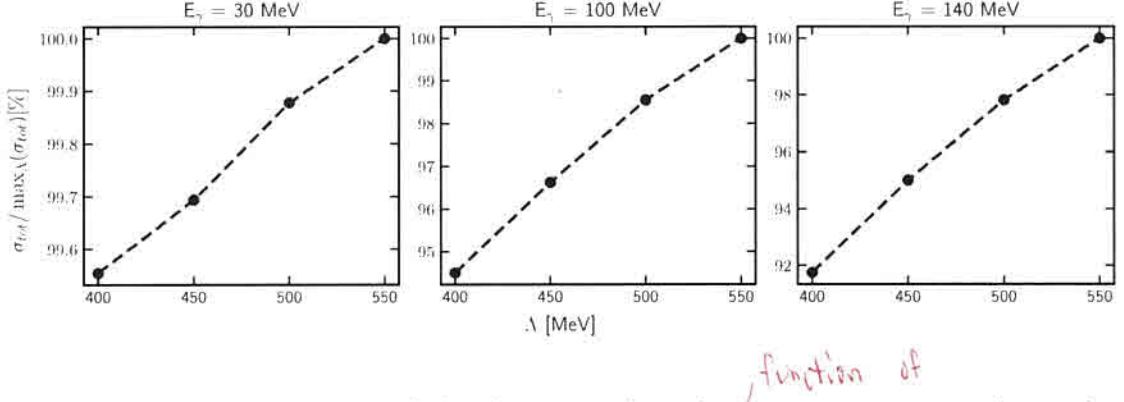


Figure 2.3: Total cross section of the deuteron photodisintegration process (normalized to the maximal cross section among all Λ) as a dependance on the cutoff parameter Λ for three photon energy E_γ values: 30, 100 and 140 MeV.

To study that I also use the same four values of the Λ parameter, obtaining in that way set of four predictions each time. That is exemplified in Fig. 2.3 for the deuteron photodisintegration cross section for the photon's energy $E_\gamma = 30 \text{ MeV}$, 100 MeV and 140 MeV . The SMS model at $N^4\text{LO}^+$ with two-nucleon force is used. Each subfigure shows predictions for the total cross section as a function of the cutoff parameter, normalized to the maximum value among all cross sections obtained with various Λ . As we can see, for that observable there is almost linear dependence with positive linearity coefficient value: with higher Λ the cross section value increases as well. Note that the higher photon's energy is, the stronger becomes the cutoff dependence: for $E_\gamma = 30 \text{ MeV}$ the maximal difference between predictions is around 0.5 % while for 140 MeV it increases to more than 8 %. These results are generally within our expectations that the chiral model works better at smaller energies and is therefore less sensitive to the Λ value. Let us remind that Λ governs the behavior of the potential at small internucleon distances and only higher energy transfer probes those distances.

Other theoretical uncertainties

There are obviously more sources of theoretical uncertainties. Our model has a number of either intrinsic limitations in precision or some simplifications which may be improved with further developments of the model.

Nuclear currents At the moment, our model is limited to a single nucleon current, which may not be sufficient to accurately describe the processes under consideration. This limitation will be further discussed and tested in Chapter 3. To address this issue, we utilize the Siegert theorem, which enables us to incorporate some contributions from the two-nucleon current, although it does not yet complete a job. It is worth noting that the incorporation of the two-nucleon current can significantly affect the predicted observables, as it includes additional physical effects that are not accounted for in the single nucleon current. Therefore, the ongoing development of a complete chiral two-nucleon current is of great importance for our model to improve the accuracy of the predictions.

Nonrelativistic approach All the results presented here does not include relativistic corrections. At the lower energies the relativistic contribution might not be crucial, but at the region with higher energy we may see a lack of precision. This will be also confirmed and discussed regarding the total cross section for the deuteron photodisintegration (see Fig. 3.2).

Uncertainties in the potential free parameters Since the chiral potential is of a semi-phenomenological type, the fitting procedure is applied in order to obtain the potential parameters [25]. The values of the free parameter of the SMS NN potential as well as free parameters of the 3N interaction have been obtained from the data by the least square fitting. As any fitting procedure, it introduces an uncertainty to the obtained values which depends on the algorithm's precision as these values are actually estimators of expectation values only. These errors, in principle, are being propagated to the observables as different set of parameters leads to a different predictions. Indeed, in [25] the whole correlation matrix for free parameters of the SMS NN force is given. Using that knowledge, it is possible to study the propagation of the uncertainty of NN force parameters to 3N observables. It is done in [65, 66] for the elastic and inelastic nucleon-deuteron scattering. Resulting uncertainties have been found to be much smaller (typically one order of magnitude) than uncertainties arising from truncation errors or cutoff dependence. I expect the same uncertainty level in electromagnetic processes and thus I do not intend to study that theoretical error in the presented thesis. Moreover, estimation of such errors is computationally expensive, since it requires significant amount of computer processing power (separate calculations for each set of parameters). In future it could be interesting to check that type of uncertainty for photodisintegration processes but it should be done after completing all pieces of Hamiltonian, specifically after including many-body electromagnetic currents.

Uncertainties from the numerical method All my results base on numerical calculations, so we can come up with a lot of places where numerical methods with limited precision come into the scene. Our approach is based on the partial wave decomposition and in practice only limited number of partial waves is included (usually for 2N scattering we use all channels up to $j^{max} = 4$ which corresponds to 18 partial waves). For 3N calculations we use $J^{max} = 15/2$ ~~32~~ which corresponds to 142 partial waves. In addition, I work with some grid of points which is used for the calculation of potential, wave function, numerical integration, etc. The choice of grid affects a final results' precision. Usually, we use a grid of ~~32~~ values which was proven to make resulting uncertainty small [17].

Model choice I focus on the SMS potential, but using another model of interaction in general leads to different predictions. That difference is also a theoretical uncertainty thus we use predictions obtained with the semiphenomenological AV18 model in order to compare the chiral results. The AV18 model is a widely used and well-established model of nuclear interaction, which has been extensively tested and benchmarked against experimental data. By comparing the predictions obtained from the SMS potential with those obtained from the AV18 model, we can assess the robustness (comparing to the AV18 results) of our results and determine the extent to which they depend on the choice of the interaction model. This comparison also helps to identify the strengths and

* Since not all ~~the chiral~~ potential parameters are ~~fixed~~ given by the theory,
the fitting ~~to~~ - data procedure is applied ...

weaknesses of each model and provides insights into the underlying physics of nuclear interactions.

Machine precision Finally, it should be noted that every computer calculation includes limited numerical machine precision which can be noticeable for complex calculations. We perform our calculations via CPU machine, where the particular choice of the processor and memory card may lead to numerical uncertainty. However, we have found that this uncertainty is much smaller than the uncertainties discussed above, and its impact on our results is negligible. We have taken great care to ensure that our calculations are performed using appropriate numerical methods and sufficient computational resources to minimize any numerical errors that may arise.

*These are done
by careful choice of Fortran compiler and compilation options.*